GEOPHYSICAL RESEARCH LETTERS, VOL. 37, L06701, doi:10.1029/2009GL042196, 2010

Rapid hydrologic shifts and prolonged droughts in Rocky Mountain headwaters during the Holocene

Bryan Shuman,[1] Paul Pribyl,[1] Thomas A. Minckley,[2] and Jacqueline J. Shinker[3]

Received 15 December 2009; revised 26 January 2010; accepted 1 February 2010; published 16 March 2010.

[1] Rapid hydroclimatic shifts repeatedly generated centuries to millennia of extensive aridity across the headwaters of three of North America's largest river systems during the Holocene. Evidence of past lake-level changes at the headwaters of the Snake-Columbia, Missouri-Mississippi, and Green-Colorado Rivers in the Rocky Mountains shows that aridity as extensive and likely as severe as the CE 1930s Dust Bowl developed within centuries or less at ca. 9 ka (thousand years before CE 1950), and persisted across large areas of the watersheds until ca. 3 ka. Regional water levels also shifted abruptly at >11.3 and 1.8-1.2 ka. The record of low water levels during the mid-Holocene on the Continental Divide links similar evidence from the Great Basin and the Midwestern U.S., and shows that extensive aridity was the Holocene norm even though few GCMs have simulated such a pattern. **Citation:** Shuman, B., P. Pribyl, T. A. Minckley, and J. J. Shinker (2010), Rapid hydrologic shifts and prolonged droughts in Rocky Mountain headwaters during the Holocene, *Geophys. Res. Lett.*, *37*, L06701, doi:10.1029/2009GL042196.

1. Introduction

[2] As global climate conditions shift away from the historic range of decadal-to-annual variability, the potential for large hydroclimatic shifts has increased with important implications for water-stressed regions like the western U.S. [e.g., *Seager et al.*, 2007]. Dendroclimatic evidence demonstrates the potential for multi-decade "megadroughts" [e.g., *Meko et al.*, 2007], but sedimentary records are needed to constrain the possibility of longer hydroclimate variations. Prolonged aridity in central North America during the mid-Holocene is well documented (Figure 1), but centennial-to-millennial hydroclimatic changes are poorly understood, particularly in the Rocky Mountains. Regional hydrologic history, however, is important for understanding past ecosystem changes [e.g., *Lynch*, 1998], ancient human populations [*Surovell et al.*, 2009], the Yellowstone caldera [*Pierce et al.*, 2002], and the variability of regional water supplies.

[3] Low lake levels existed during the Holocene in the Rocky Mountains [e.g., *Shuman et al.*, 2009] (Figure 1b), but the magnitudes and rates of the attendant hydroclimate changes have not been quantified or consistently well dated. Additionally, regional aridity has not been uniformly recognized. In one data synthesis, five of the seven fossil pollen records from >2500 meters in the Rocky Mountains interpreted to show moisture differences from today indicate high moisture levels at 6 ka [*Harrison et al.*, 2003]. Likewise, multiple models demonstrate the possibility of high regional precipitation at 6 ka [*Braconnot et al.*, 2007; *Harrison et al.*, 2003; *Shin et al.*, 2006], although one regional simulation produced severe aridity [*Diffenbaugh et al.*, 2006].

[4] Here, we examine the history of water supplies at the convergence of three major North American watersheds: the Snake-Columbia, Bighorn-Missouri-Mississippi, and the Green-Colorado River basins. To do so, we reconstruct water-level changes at Lake of the Woods (43.48 N, 109.89 W, 2816 m elevation, 42 ha area) located where the watersheds meet in Wyoming (Figure 1a). We then assume that past changes in lake volume equal changes in the balance of watershed inputs and outflow to provide a quantified hydroclimatic history.

2. Study Site

[5] A depression in glacial till forms Lake of the Woods (LOW), which has a well-defined watershed (180 ha (Figure 1b)) in subalpine parkland with little to no external groundwater inputs (given its high topographic position). The lake is dilute (25 μm conductivity), has no outlet or other stream connections, and has depths to 11 m (see auxiliary material for bathymetric map).[4] The watershed divide coincides with the Continental Divide north of the lake, and varies in elevation above the lake by 1–19 m. No known geomorphic evidence indicates ancient high stands or periods of overflow.

3. Approach

[6] The past shoreline elevations of LOW were determined from ground-penetrating radar (GPR) profiles and sediment cores (Figures 2 and 3). Our reconstruction is based on the concepts that sandy sediments typically accumulate near lake margins, and that continuous accumulation of organic silt only takes place in relatively deep water. Wave energy in shallow water keeps total sediment (particularly silt and mud) accumulation to a minimum. Sediment sequences at the margin of lakes, therefore, can contain alternating layers of 1) sand with low net accumulation rates and 2) organic silts with high net accumulation rates associated with low and high water periods respectively.

[1]Department of Geology and Geophysics, University of Wyoming, Laramie, Wyoming, USA.
[2]Department of Botany, University of Wyoming, Laramie, Wyoming, USA.
[3]Department of Geography, University of Wyoming, Laramie, Wyoming, USA.

0094-8276/10/2009GL042196

[4]Auxiliary materials are available in the HTML. doi:10.1029/2009GL042196.

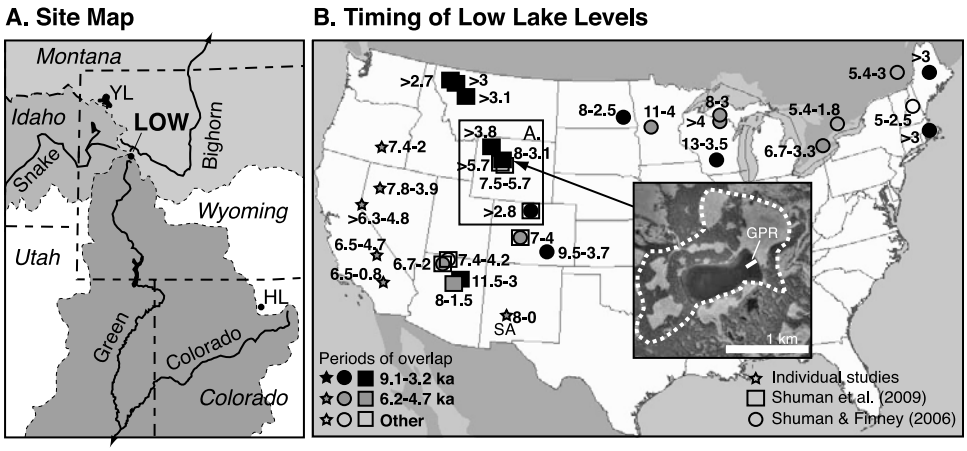

Figure 1. Study location, aerial photo, and hydroclimatic context. (a) Site locations are shown within the Green-Colorado (dark gray), Snake-Columbia (intermediate gray), and Upper Missouri (light gray) watersheds. Lakes discussed here are labeled: Lake of the Woods (LOW), Yellowstone Lake (YL) and Hidden Lake (HL). (b) Representative lake-level data indicate periods of low water from the Rocky Mountains to the Great Lakes at ca. 9-3 ka (black symbols), from California to Ontario at ca. 6.2-4.7 ka (black and gray symbols), and from California to Maine from ca. 4.7-3 ka. Data were compiled from two reviews (squares and circles [*Shuman and Finney*, 2006; *Shuman et al.*, 2009]), and from other individual studies (stars [*Adams et al.*, 2008; *Bacon et al.*, 2006; *Benson et al.*, 2002; *Briggs et al.*, 2005; *Dugas*, 1998; *Markgraf et al.*, 1984; *Negrini et al.*, 2006]). Inset aerial photograph shows LOW with lines denoting its watershed (dashed) and GPR profile location (solid (Figure 2)).

[7] Here, we infer periods of low water from dense packets of sandy sediment that 1) extend out from shore nearly continuously around the lake margin, 2) interrupt units of organic silts and mud, and 3) have low net sedimentation rates (i.e., ~10 cm/ka or less based on *Webb and Webb* [1988]). Paleoshorelines are thus differentiated from other potential sedimentary features, such as aeolian, mass movement or flood deposits, which form localized layers of coarse sediment with high net accumulation rates. The low angle of the watershed and littoral slopes near the core locations (1.6% and 0.5% respectively), and a lack of nearby aeolian sediment sources, also limits the possibility of these alternatives. Relative elevations of sand and silt layers differentiate the effects of water-level change and sediment infilling. Sediment infilling raises the lake bottom into the zone of wave action and can enable sands to extend laterally over silts at a constant elevation (i.e., above the wave base), but water-level changes can raise or lower the elevation of the boundary between silts and sands. We infer changes in lake level from such shifts (Figures 3 and 4).

4. Methods

[8] GPR data were obtained in CE 2008 using a GSSI, Inc. SIR-3000 GPR with 200 and 400 MHz antennae floated on the lake surface in an inflatable boat. Data in Figure 2 were collected using the 400-MHz antenna, and are representative of >10 profiles collected around the lake margin. A transect of sediment cores was collected with a piston corer in the same year. Contiguous 1-cm sediment samples from core 2A were wet sieved through a 63 μm mesh, and the residual sediment was weighed after ignition at 500°C to determine the inorganic coarse sediment (sand) content. To correlate sand layers among cores, we use bulk density logs

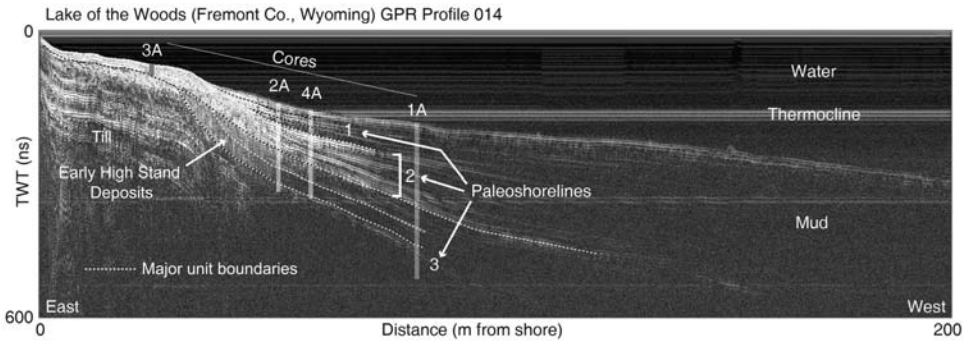

Figure 2. Ground-penetrating radar (GPR) profile showing submerged paleoshorelines at Lake of the Woods. Vertical scale shows the two-way travel time (TWT) of the radar signal in nanoseconds (ns), and is approximately equal to 6 meters. Vertical bars show core locations (Figure 3). Numbers denote sediment packets interpreted as paleoshorelines.

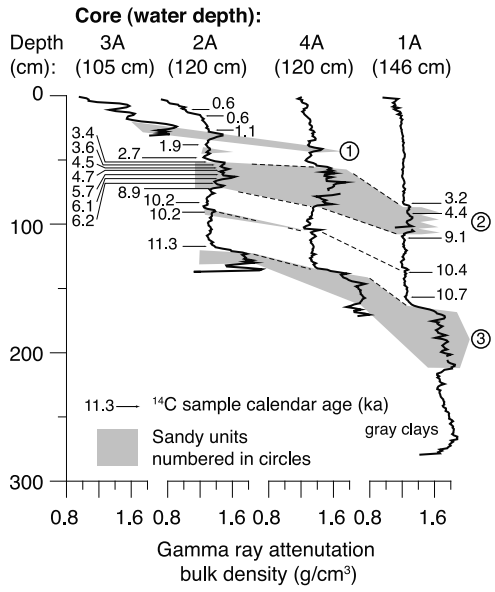

Figure 3. Sediment bulk density and radiocarbon data for cores collected at Lake of the Woods indicate the depths and median ages of paleoshorelines. Gray shading denotes the dense minerogenic sediment packets interpreted to be paleoshorelines (circled numbers).

generated by gamma-ray attenuation on a Geotek, Inc. Multi-Sensor Core Logger.

[9] Sedimentary charcoal (>125 μm) was extracted above and below sand layers for radiocarbon analyses. The ages indicate net sedimentation rates and the chronology of the inferred lake-level changes. The dates were calibrated to calendar years using CALIB 5.0 [*Reimer et al.*, 2004]. The 1σ ranges of the calendar ages are shown here rounded to the nearest decade (see also auxiliary material).

[10] We estimate changes in the balance of precipitation and evapotranspiration (ΔP-E) from the lake-level history, but the separate effects of P and E across the lake and watershed cannot be isolated. We first estimate changes in lake elevation (ΔElev) from changes in the elevation of the sand-silt boundary, and assume that the water depth of the boundary (~100 cm today) has remained unchanged. We then calculate changes in lake volume (ΔV_L) by accounting for lake area (A_L), and divide by the combined watershed and lake area (A_W) to estimate the equivalent total P-E (in mm). Finally, we divide by the lake-climate equilibration time (ΔT) to obtain a ΔP-E value in mm/day based on the following equation:

$$\Delta V_L = (\Delta Elev * A_L) = \Delta P - E * A_W * \Delta T$$

We present ranges of ΔP-E derived by varying ΔT from 182.5 days (0.5 years) to 1825 days (5 years) consistent with equilibrium response times for hydrologically-open lakes [*Mason et al.*, 1994]. The mean and standard deviations of the repeated calculations (n=46 per value of ΔElev) are presented here. We assume that groundwater leakage has remained constant through time, but reduced hydrostatic head during low water should reduce groundwater outflow and make our ΔP-E estimates conservative. Sediment thicknesses above each sand layer indicate that bathymetric evolution via sediment infilling could have reduced subsequent ΔV_L values by ~20%, but any effect on our calculations is likely smaller than unincorporated changes in the watershed groundwater volume, which would increase our ΔP-E estimates (possibly by >130% based on the watershed size, changes in groundwater level equal to ΔElev, and an assumed till porosity of 40%).

5. Lake-Level Changes

[11] GPR profiles from LOW (Figure 2) show several packets of bright radar reflectors extending out from shore, which correspond to dense, sandy intervals amid silts in our sediment cores (Figure 3). The uppermost packet (1) lies between calibrated radiocarbon ages of 1.89-1.83 and 1.17-1.07 ka in core 2A. The middle sedimentary packet of dense sands (2) is bracketed by dates of 9.00-8.78 and 3.47-3.41 ka in core 2A and by dates of 9.13-9.03 and 3.24-3.08 ka in core 1A. Packet 3 was deposited before 11.34-11.26 ka.

[12] Net sedimentation rates associated with the sands were consistently low (<12 cm/ka (Figure 4b)) relative to inter-bedded silts (12-21 cm/ka), and dropped to 1.9 cm/ka in the bottom of packet 2 (ca. 8.9-6.2 ka), which correspondingly has the most extensive GPR reflectors. Because the sand and associated low net accumulation rates extend furthest out from shore, packet 2 probably represents the lowest Holocene water level. Water currently covers these features despite severe regional drought from CE 1998–2007, and they likely represent historically unprecedented reductions in water supply: either consistently low water or

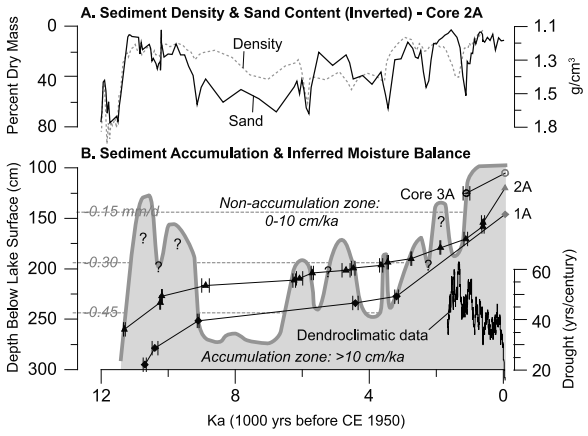

Figure 4. Lake of the Woods water levels, based on sediment sand content and net sediment accumulation rates, compared with dendroclimatic evidence [*Cook and Krusic*, 2004]. (a) Sediment density (dashed line) and sand content (solid line) of core 2A tracks the lake-level history (B) as inferred from shifts in the extent of the lake's accumulation zone (where sediments accumulated at >10 cm/ka). (b) Gray line shows the maximum elevation of the sediment accumulation zone based on the age-depth relationships of cores 1A (diamonds), 2A (triangles), and 3A (open circles). Closed symbols indicate AMS radiocarbon ages, open symbols indicate points of stratigraphic correlation, and gray symbols indicate the core tops. Dashed lines denote the mean ΔP-E, and the black line at the lower right shows the frequency of regional drought (years with Palmer Drought Severity Index of −1 or less) based on a local reconstruction using >3 tree-ring chronologies [*Cook and Krusic*, 2004].

frequent annual-to-decadal droughts. Silts below packet 2 (with <20% sand (Figure 4a)) extend shoreward of core 2A (Figure 2), and indicate early levels that were higher than after ca. 9 ka, if not as high as today.

[13] Water levels appear to have shifted rapidly at several intervals, such as at ca. 9 and 1.5 ka when sand content changed abruptly by >20% at the base of packets 1 and 2 (Figure 4a). Because packet 2 was deposited immediately above ages of 9.00-8.78 and 9.13-9.03 ka in cores 2A and 1A respectively (Figure 3), the lake likely fell by >60 cm (ΔP-E: 0.21 ± 0.16 mm/day) within the age range of the dates. Packet 3 indicates a similar magnitude change following the Younger Dryas cool interval [e.g., *MacDonald et al.*, 2008].

[14] Other evidence confirms our interpretations. Packet 1 formed during a period of >50 drought yrs per century at 1.38-1.29 ka, based on years with Palmer Drought Severity Index below −1 in a reconstruction from northwest Wyoming (Figure 4b) [*Cook and Krusic*, 2004]. Packet 2 overlaps in time with sedimentary hiatuses (possibly indicative of desiccation at ca. 8.0-3.1, >5.7, and 7.5-5.7 ka) at three near-by kettle ponds [*Lynch*, 1998]. A paleoshoreline 5 m below the surface of Yellowstone Lake (YL) also dates to >4.04-3.69 ka [*Pierce et al.*, 2002], which is synchronous with the timing of packet 2. YL paleoshorelines relate to local tectonism [*Pierce et al.*, 2002], but packet 2 provides evidence that severe aridity could have also contributed to YL's complex history. The severity of the Holocene droughts may also well explain why human populations were nearly absent from northern Wyoming at ca. 9-6 ka [*Surovell et al.*, 2009].

[15] Low water periods at LOW also coincide with those at lakes across the Rocky Mountains [*Shuman et al.*, 2009] and North America generally [*Shuman and Finney*, 2006]. Lakes from Arizona to Wisconsin were low from ca. 9.1-6.2 ka (black symbols (Figure 1b)). From ca. 6.2-4.7 ka, the aridity extended from California to Ontario (gray symbols (Figure 1b)), and then until <3.2 ka extended east to Maine (Figure 1b), coincident with the uppermost sand in Unit 2.

6. Moisture-Balance Estimates

[16] Holocene aridity was likely as severe as historic droughts, such as the CE 1930s when ΔP-E in the Great Plains was near −0.2 mm/day [*Schubert et al.*, 2004]. The mean ΔP-E from today required for LOW to occupy its paleoshorelines must have exceeded −0.67 ± 0.52 mm/day before ca. 11.3 ka (>200 cm lower water level than today), −0.50 ± 0.39 mm/day from ca. 9.0-3.4 ka (>150 cm lower), and −0.15 ± 0.12 mm/day at ca. 1.8-1.1 ka (>45 cm lower). Using the same approach, we calculate that low shorelines at Hidden Lake, Colorado from 8.4-4.4 ka [*Shuman et al.*, 2009] could have resulted from ΔP-E of −0.35 ± 0.27 mm/day. Both reconstructions are consistent with regional climate model simulations of ΔP-E at 6 ka of 0.3–0.5 mm/day for Colorado and Wyoming [*Diffenbaugh et al.*, 2006], but our results differ from high precipitation rates simulated by GCM studies (including those by *Diffenbaugh et al.* [2006]) and reconstructed from pollen [e.g., *Harrison et al.*, 2003]. The differences may depend on important fine-scale climate dynamics not captured by the GCMs, as well as temperature effects and seasonal precipitation.

7. Conclusions

[17] The headwaters of the largest river systems in the western U.S. experienced prolonged and severe drought, and rapid hydrologic change, during the Holocene with implications for river flows, ecosystem history, and human history. The past hydroclimate shifts underscore the potential for rapid hydroclimate changes when global to regional climate drivers change.

[18] **Acknowledgments.** Funding provided by the USGS and Wyoming Water Development Commission grants (06HQGR0129 and WWDC25) to B.S., J.S., and T.M., and by NSF (EPS-0447681) including for a Wyoming EPSCoR undergraduate fellowship to P.P.

References

Adams, K. D., et al. (2008), Late Pleistocene and early Holocene lake-level fluctuations in the Lahontan Basin, Nevada: Implications for the distribution of archaeological sites, *Geoarchaeology*, *23*(5), 608–643, doi:10.1002/gea.20237.

Bacon, S. N., et al. (2006), Last Glacial Maximum and Holocene lake levels of Owens Lake, eastern California, USA, *Quat. Sci. Rev.*, *25*(11–12), 1264–1282, doi:10.1016/j.quascirev.2005.10.014.

Benson, L., et al. (2002), Holocene multidecadal and multicentennial droughts affecting northern California and Nevada, *Quat. Sci. Rev.*, *21*(4–6), 659–682, doi:10.1016/S0277-3791(01)00048-8.

Braconnot, P., et al. (2007), Results of PMIP2 coupled simulations of the mid-Holocene and Last Glacial Maximum—Part 1: Experiments and large-scale features, *Clim. Past*, *3*, 261–277.

Briggs, R. W., et al. (2005), Late Pleistocene and late Holocene lake highstands in the Pyramid Lake subbasin of Lake Lahontan, Nevada, USA, *Quat. Res.*, *64*(2), 257–263, doi:10.1016/j.yqres.2005.02.011.

Cook, E. R., and P. J. Krusic (2004), The North American drought atlas, Lamont-Doherty Earth Obs., Palisades, N. Y. (Available at http://iridl.ldeo.columbia.edu/expert/SOURCES/.LDEO/.TRL/.NADA2004/.pdsi-atlas.html)

Diffenbaugh, N. S., M. Ashfaq, B. Shuman, J. W. Williams, and P. J. Bartlein (2006), Summer aridity in the United States: Response to mid-Holocene changes in insolation and sea surface temperature, *Geophys. Res. Lett.*, *33*, L22712, doi:10.1029/2006GL028012.

Dugas, D. P. (1998), Late Quaternary variations in the level of paleo-Lake Malheur, eastern Oregon, *Quat. Res.*, *50*(3), 276–282, doi:10.1006/qres.1998.2005.

Harrison, S. P., et al. (2003), Mid-Holocene climates of the America: A dynamical response to changed seasonality, *Clim. Dyn.*, *20*, 663–688.

Lynch, E. A. (1998), Origin of a park-forest vegetation mosaic in the Wind River Range, Wyoming, *Ecology*, *79*(4), 1320–1338.

MacDonald, G. M., et al. (2008), Evidence of temperature depression and hydrological variations in the eastern Sierra Nevada during the Younger Dryas stade, *Quat. Res.*, *70*(2), 131–140, doi:10.1016/j.yqres.2008.04.005.

Markgraf, V., et al. (1984), San Agustin Plains, New Mexico: Age and paleoenvironmental potential reassessed, *Quat. Res.*, *22*(3), 336–343, doi:10.1016/0033-5894(84)90027-9.

Mason, I. M., M. A. J. Guzkowska, C. G. Rapley, and F. A. Street-Perrott (1994), The response of lake levels and areas to climatic change, *Clim. Change*, *27*, 161–197, doi:10.1007/BF01093590.

Meko, D. M., C. A. Woodhouse, C. A. Baisan, T. Knight, J. J. Lukas, M. K. Hughes, and M. W. Salzer (2007), Medieval drought in the upper Colorado River Basin, *Geophys. Res. Lett.*, *34*, L10705, doi:10.1029/2007GL029988.

Negrini, R. M., et al. (2006), The Rambla highstand shoreline and the Holocene lake-level history of Tulare Lake, California, USA, *Quat. Sci. Rev.*, *25*(13–14), 1599–1618, doi:10.1016/j.quascirev.2005.11.014.

Pierce, K. L., et al. (2002), Post-glacial inflation-deflation cycles, tilting, and faulting in the Yellowstone Caldera based on Yellowstone Lake shorelines, *U.S. Geol. Surv. Open File Rep.*, *02-0142*, 30 .

Reimer, P. J., et al. (2004), IntCal04 terrestrial radiocarbon age calibration, 26–0 ka BP, *Radiocarbon*, *46*, 1026–1058.

Schubert, S. D., M. J. Suarez, P. J. Pegion, R. D. Koster, and J. T. Bacmiester (2004), On the causes of the 1930s Dust Bowl, *Science*, *303*(5665), 1855–1859, doi:10.1126/science.1095048.

Seager, R., et al. (2007), Model projections of an imminent transition to a more arid climate in southwestern North America, *Science*, *316*(5828), 1181–1184, doi:10.1126/science.1139601.

Shin, S.-I., P. D. Sardeshmukh, R. S. Webb, R. J. Oglesby, and J. J. Barsugli (2006), Understanding the mid-Holocene climate, *J. Clim.*, *19*, 2801–2817, doi:10.1175/JCLI3733.1.

Shuman, B., and B. Finney (2006), Late-Quaternary lake-level changes in North America, in *Encyclopedia of Quaternary Sciences*, edited by S. Elias, pp. 1374–1383, Elsevier, Amsterdam.

Shuman, B., et al. (2009), Holocene lake-level trends in the Rocky Mountains, U.S.A., *Quat. Sci. Rev.*, *28*(19–20), 1861–1879, doi:10.1016/j.quascirev.2009.03.003.

Surovell, T. A., et al. (2009), Correcting temporal frequency distributions for taphonomic bias, *J. Archaeol. Sci.*, *36*(8), 1715–1724, doi:10.1016/j.jas.2009.03.029.

Webb, R. S., and T. Webb III (1988), Rates of sediment accumulation in pollen cores from small lakes and mires of eastern North America, *Quat. Res.*, *30*(3), 284–297, doi:10.1016/0033-5894(88)90004-X.

T. A. Minckley, Department of Botany, University of Wyoming, 1000 University Ave. Laramie, WY 82071, USA.

P. Pribyl and B. Shuman, Department of Geology and Geophysics, University of Wyoming, 1000 University Ave. Laramie, WY 82071, USA. (bshuman@uwyo.edu)

J. J. Shinker, Department of Geography, University of Wyoming, 1000 University Ave. Laramie, WY 82071, USA.